

# NEW TRENDS IN DEVELOPMENT OF MAGNETIC-FIELD BRAGG-GRATING FIBER OPTIC SENSORS BASED ON MAGNETIC NANOFLUIDS

<sup>1</sup>Jozef Jasenek, <sup>2</sup>Jozefa Červeňová, <sup>3</sup>Branislav Korenko

<sup>1,2,3</sup> Institute of Electrical Engineering, FEI STU Bratislava, Ilkovičova 3, 812 19 Bratislava  
E-mail: Jozef.Jasenek@stuba.sk, [Branislav.Korenko@stuba.sk](mailto:Branislav.Korenko@stuba.sk), Jozefa.Cervenova@stuba.sk,

Received 24 April 2014; accepted 06 May 2014

## 1. Introduction

Except of the traditional use of optical fibers for information signal transmission they are now broadly applied also in sensing applications [1]. A lot of various physical quantities can be measured locally or as distributed in space along the sensing optical fibre [2]. So we can speak about the local fibre optic sensors (FOS) or space distributed FOS. Due to the rather high sensitivity and space resolution of these sensors their importance is significant and the amount of investment into this field is growing rapidly worldwide [3]. Special group of these sensors concerns the measurement of the magnetic field (MF). At present many approaches to the solution and design of FO MF sensors do exist [1, 4]. One of the most important ways how to use the OF for the MF sensing is the exploration of the fluids infiltrated with magnetic nanoparticles [5]. The magnetic fluids (MFL) with a suitable concentration of magnetic nanoparticles when coming into contact with the fibre can significantly change the propagation modes characteristics in the core and the cladding. These changes can be put into relation with the magnitude of external MF and detected using different approaches. In this contribution we map some of modern trends in the utilization of microstructured OF in combination with magnetic fluids for the design of the MF FOS.

## 2. MFS based on the use of birefringent dual "hollow-core" PCF filled with MFL

One of the attractive possibilities for construction of the FOS for sensing of MF is the use of a piece of the dual "hollow core" photonic crystal fiber (HC-PCF) filled with the MFL.

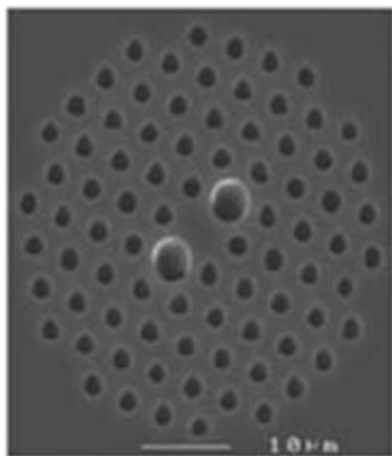


Fig. 1 Dual core birefringent HC-PCF

Such an optical fiber, see Fig. 1, when filled-in with a suitable MFL, changes its birefringence properties depending on the magnitude of the applied external MF. The simplified scheme of the experimental setup for realization of such a sensor is depicted in the Fig. 2. It consists of a broad band tuneable optical source OS and optical detector OD which are connected to the input and output of the birefringent optical HC-PCF. There are also two linear polarizers LP1, LP2 for adjustment of the input radiation polarization and for the detection of the output signal influenced by the birefringence change in the HC-PCF induced by external magnetic field to be measured [6].

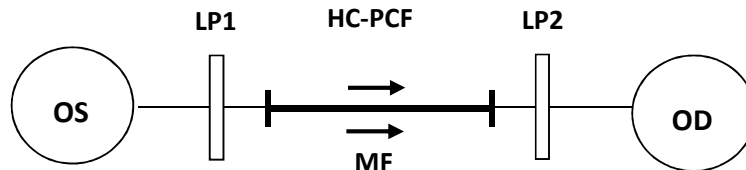


Fig. 2 The simplified scheme of the experimental setup

The nanofluid can be infiltrated inside PCF air holes by using e. g. syringe with a suitable diameter needle. More of nanofluid infiltrates inside the core holes with diameter cca 4.5  $\mu\text{m}$  as compared with infiltration to smaller holes of diameter cca 2.2  $\mu\text{m}$ . Measurement setup works on the principle of birefringent interferometer using a piece of birefringent HC-PCF of length cca 23.5 cm that is connected between two in-line fiber polarizers. In order to apply a magnetic field HC-PCF is kept in magnetic field generated by axial solenoid which provides magnetic field variation from 0 to cca 80 mT. The measured output intensity spectrum of the birefringent HC-PCF can be described by the transmission function

$$H(\lambda) = \cos^2(2\pi BL/\lambda) \quad (1)$$

where  $B$  represents intrinsic birefringence defined by the relation  $B=(n_s-n_f)$  what is the difference of the effective refractive indices (RI)  $n_s$  and  $n_f$  pertaining to the slow and fast axis of a HC-PCF, respectively. The wavelength difference between the neighbouring interference dips of transmission spectra strongly depends on HC-PCF birefringence. It can be described by the relation  $\Delta\lambda=\lambda^2/BL$  where  $\Delta\lambda$  is the wavelength difference between two minima or maxima,  $L$  is the HC-PCF length. The transmission function  $H(\lambda)$  depends on  $B$ , that is directly dependent on the external magnetic field. The influence of external MF on infiltrated HC-PCF results in MF dependent total birefringence defined by  $B = (n_s - n_f) - (n_{sm} - n_{fm})$  where  $n_{sm}$  and  $n_{fm}$  are the effective RI induced by applied MF. Increasing applied MF causes a shift of the wavelength dips to lower wavelengths as shown in the Fig.3. It can be explained by the birefringence reduction caused by increasing MF.

The chosen wavelength dip at 1570 nm has been tracked and the variation of that dip as a function of applied MF is shown in Fig. 4 for two concentrations of nanofluid - 0.3 mg/ml and 0.6 mg/ml. The wavelength shift as a function of applied MF is linear in the range of 0-45 mT as it is shown in the inset. Corresponding measurement sensitivities for the  $\text{Fe}_3\text{O}_4$  concentrations of 0.6 mg/ml and 0.3 mg/ml are 242 pm/mT and 155.7 pm/mT respectively. The wavelength shift at higher magnetic fields is rather nonlinear. This figure also clearly shows that magnetic field sensitivity depends on nanofluid concentration.

This type of OF MFS consisting of dual HC-PCF infiltrated with other more suitable MFL makes possible to measure MF with higher sensitivities than those for 155.7 pm/mT and 242 pm/mT for 0.3 mg/ml and 0.6 mg/ml concentration of  $Fe_3O_4$ , respectively.

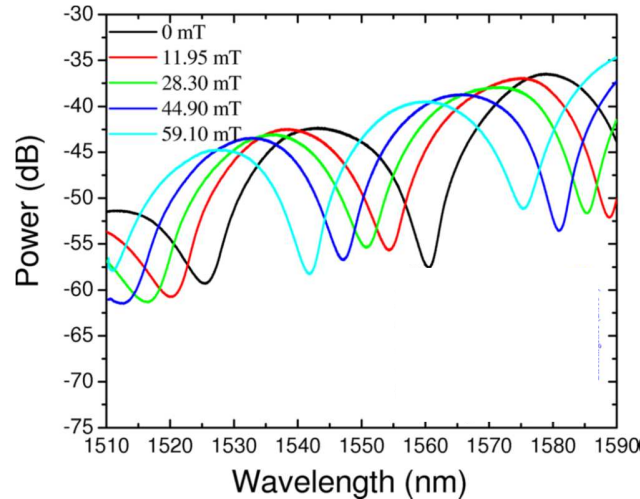


Fig. 3 Fringe pattern of HC-PCF filled with 0.6 mg/ml concentrated  $Fe_3O_4$  nanofluid at different magnetic fields.

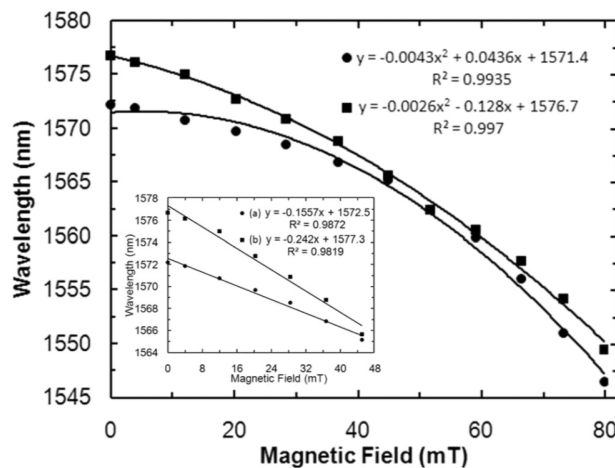


Fig.4 Magnetic field response of HC-PCF in terms of wavelength shift for (a) 0.3 mg/ml and (b) 0.6 mg/ml concentrated  $Fe_3O_4$  nanofluid. Inset shows the linear response.

### 3. MFS based on the use of the "index-guiding" PCF filled with MFL

In this approach a section of "index guiding PCF" (IG-PCF) filled with MFL is used. The fiber core diameter is cca 7  $\mu\text{m}$ , the cladding hole diameter is 2,57  $\mu\text{m}$ . The separation distance between the holes is 5,12  $\mu\text{m}$ , Fig. 5. In contrast with beforegoing HC PCF only cladding capillaries are filled with MFL and therefore the situation now is quite different.

Applied external MF causes the difference of the effective RI between the fiber core and the cladding. The changes of the applied MF are now related to the measured transmission loss. The used MFL is a water-based ferrofluid prepared by precipitation technique [7]. The nominal diameter of the nanoparticles of  $Fe_3O_4$  is 9 nm. Oleic acid is used to disperse the solid-state

nanoparticles in an appropriate solvent uniformly. According to Fig. 6, the refractive index  $n_{MF}$  at MF cca (43x80) A/m begins to change and is saturated at a magnitude of cca 604x80 A/m. Increasing external MF causes the reduction of RI difference between the fiber core and the cladding space. As a result the energy of the radiation propagating in the fiber core is partially transferred into the cladding space. Effective RI of the cladding is now represented by a complex number.

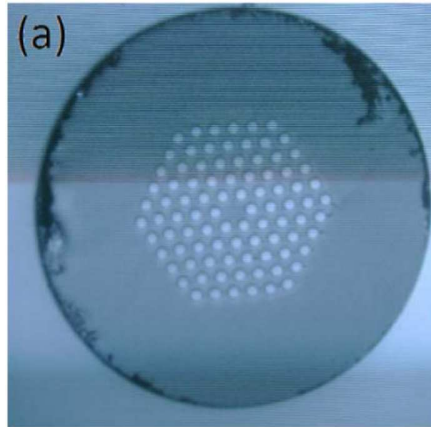


Fig. 5 Scanning electron microscope image of cross section of the used IG-PCF

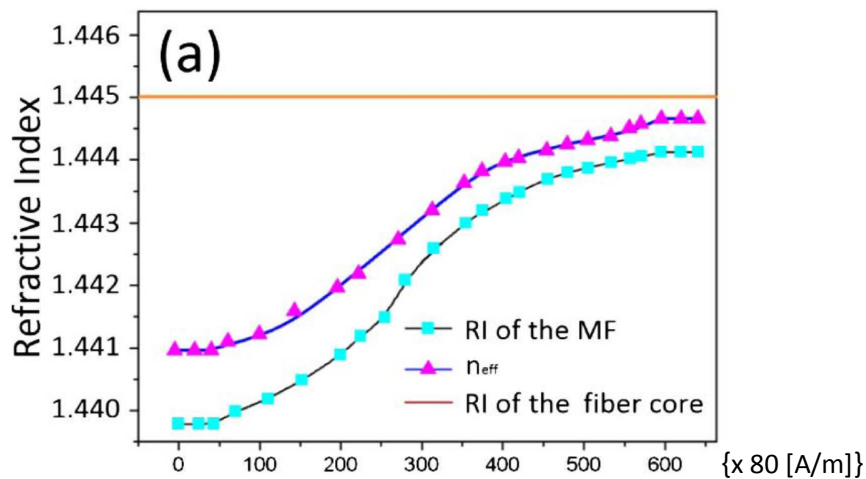


Fig. 6 RI dependences on MF

The transmission loss  $P_L$  is therefore described by the relation  $P_L = 20 \log_{10} e \cdot k_0 \cdot [\text{Im}\{n_{eff}(H)\}L]$ , where  $e=2,71828$ ,  $k_0 = 2\pi/\lambda$  and  $\lambda$  is the light wavelength,  $H$  is the intensity of applied MF and  $L$  is the length of the sensing fiber. The smaller the RI difference between the liquid in holes and the liquid in the core the larger the complex part of the  $n_{eff}(H)$ , [8]. As a consequence we can detect the magnetic field by measuring the transmission loss, Fig. 7. The laser source (LS) and the optical power meter (PM) are connected to the sensing IG-PCF through the two spliced SM optical fibers. The MF orientation is now perpendicular to the light propagation direction in the MFL-filled IG-PCF. The transmission intensity is measured by a high sensitive optical PM. The resolution of the sensor is characterised as shown in Fig.8.

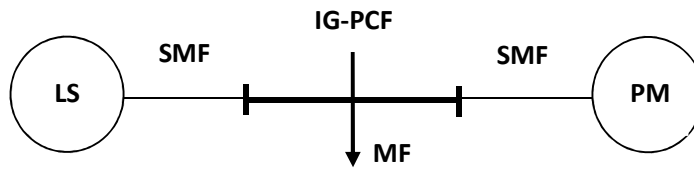


Fig. 7 The sensor simplified scheme

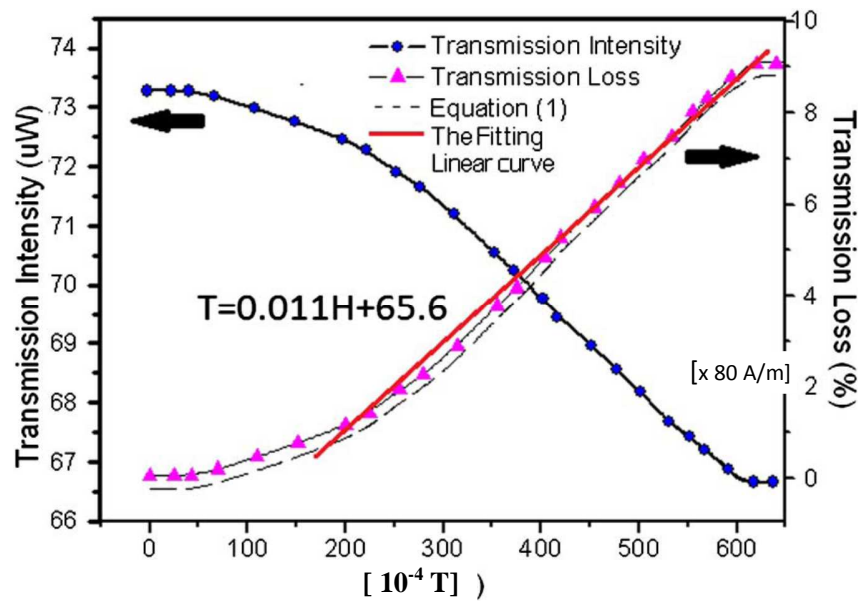


Fig. 8 Transmission intensity and transmission loss dependence on the external MF

For MF higher than  $(80 \times 200 = 1600)$  A/m the transmission intensity as a function of MF is nearly linear. Measured results indicate that the MF sensitivity of the sensor is  $(0.011/80) \mu\text{W}/(\text{A}/\text{m})$ . The proposed method possesses high sensitivity and rather low cost.

#### 4. MFS based on the use of Bragg Grating PCF (BG PCF) partially filled-in with MFL

The functionalities of infiltrated PCFs can be further augmented except of being infused with nanoparticles also by exploring the Bragg gratings (BG) [9]. This can be achieved through the influencing of physical properties and spatial position of the infiltrated media what makes possible to develop new in-fiber sensors. Recently new magnetically tuneable BG-IG-PCF was infiltrated with MFL inside their capillaries [10]. It induced a strong local phase and absorption effect and formed a Fabry–Perot resonator [11]. This resulted in the creation of the parasitic notch modes that can be detected in reflection spectra. However it is dependent on physical parameters of the placed MFL piece and its relative position along the BG-PCF.

A special grapefruit shape Ge-doped core BG-IG-PCF was infiltrated with the Ferrotec, oil-based MFL with the saturation magnetization of 0,400 T. A short length (cca 1 mm) of MFL

was infiltrated inside the fiber and translated toward the grating vicinity using a special magnet. Then it was placed at a specific point on the BG-IG-PCF creating a loss Fabry–Perot cavity. The BG-IG-PCF device contains a 9.4 mm long BG. The magnetic defect is immobilized at a specific location along the BG length to maximize the spectral contrast of the parasitic spectral notch observed in the reflection. Immobilization of defect is done by sealing one end of the BG-IG-PCF with suitable glue. This creates a closed-air cavity allowing the MFL partially to move its optimum immobilization point with the MF. The BG-IG-PCF cavity length created using this procedure is  $\sim 9$  cm. Under the application of the MF along the BG-IG-PCF axis the MFL moves along the BG length and induces measurable changes at the induced Fabry–Perot spectral notch in the reflection, Fig.9

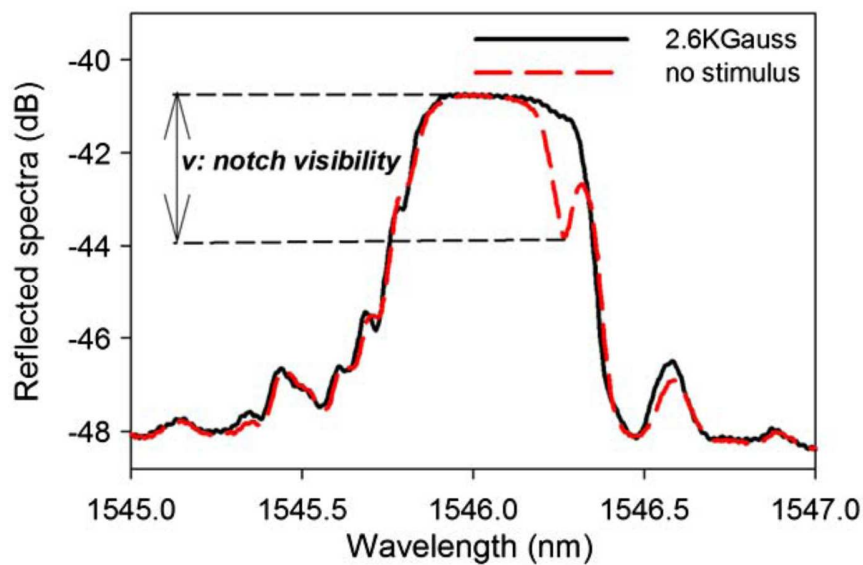


Fig. 9 Spectral response of the MFL phase defected BG-PCF for two MF states. Visibility  $v$  is defined in the spectra.

The maximum notch visibility  $\Delta v$  obtained in that case is  $\sim 3.1$  dB with respect to immobilization point. The BG-IG-PCF is fixed on a brass plate and neodymium magnet moves backward and forward along the fiber what stimulates the movement of MFL defect in the fiber. A small flux magnetometer at the immobilization point of the ferrofluid measures the actual MF to perform the calibration. The response of the described BG-IG-PCF magnetometer with different MFL versus the MF is given in Fig.10

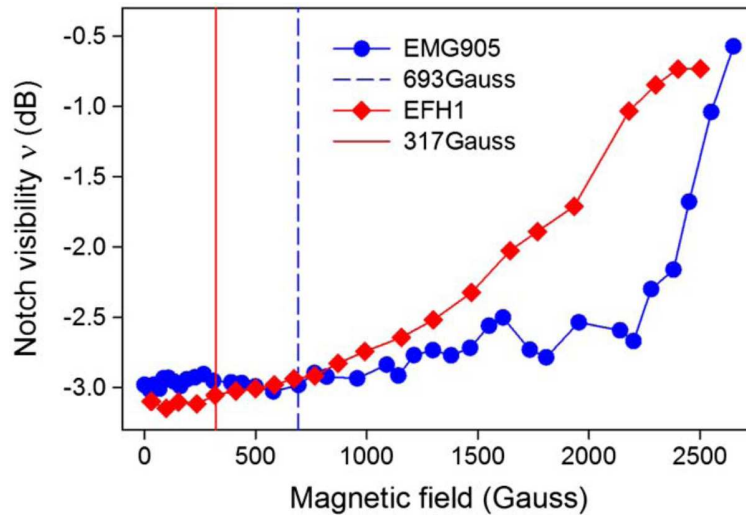


Fig.10 Notch visibility  $v$  changes resulting from the movement of the MFL defect into the BG-PCF versus the MF applied along the fiber axis for two different MFL infiltrated. Vertical lines denote the measurement sensitivity threshold for each device.

Above threshold first ferrofluid sensor shows linear like behaviour versus the MF. The threshold of that MFL sensor is estimated at 0,0317 T, and the threshold for the second MFL sensor increases by 2.18 times, to 0,0693 T. The described miniature in-fiber magnetometer utilizing BG-IG-PCF infiltrated by a short MFL defect can measure magnetic fields between 0,0317 and 0,2500 T with high precision.

## 5. Conclusion

The MF OFS are becoming very important for many practical applications due to their high available sensitivities, measurement range, small dimensions and also relatively low realization cost. Especially the MF FOS utilizing special OF like IG-PCF or HC-PCF combined with BG and simultaneously infiltrated with suitable MFL are very attractive and a significant effort to their analysis and design is devoted worldwide. We have brought a brief analysis and summary description of five approaches to the solution of the MF OFS based on the use of:

1. dual HC-PCF infiltrated with MFL where fiber exposition to the external MF induces the change of the total birefringence. As a result the minimum fringe wavelength shift of transmission intensity is measured as a function of external MF. The measurement sensitivities 155,7 – 242 pm/mT are achieved.
2. IG-PCF infiltrated with MFL and transmission losses are measured as a function of external MF. Sensitivity of cca (0,011/80)  $\mu\text{W}/(\text{A}/\text{m})$  are obtained.
3. IG-PCF with inscribed BG and partially filled in with a MFL so that OF Fairy-Perrot resonator is created and the changes in reflection spectra (notch visibility) are measured as function of external MF. The MF in the range of 0,0317 – 0.250 T can be measured by this sensor. Finally – all above described approaches can be further optimized by adjusting of several parameters of the particular structure. Therefore there is a lot of possibilities to further perfection of this kind of MF FOS mainly by the tuning of MFL composition, by optimization of the geometrical parameters of OF used and also by the inventing and finding of new structures and basic ideas.

## Acknowledgement

This work was supported by the Slovak Research and Development Agency (APVV) under the contract No. APVV-0062-11

## References

1. [1] - Fiber Optic Sensors – 2-nd Edition, Edited by S. Yin, P. B. Ruffin, F.T.S. Yu, CRC Press, Taylor and Francis Group, ISBN 978-1-4200-5365-4, Printed in USA, 2010
2. [2] – J. Jasenek. Optical Fiber Reflectometry, Slovak University of Technology, 2004, ISBN 80-227-2002-X
3. [3] - Global Optoelectronics Industry Market Report and Forecast, Optoelectronics industry Development Association (OIDA), 2009
4. [4] - Jozef Jasenek, Branislav Korenko, Jozefa Červeňová, Jaroslav Erdziak: Fiber Optic Magnetic Field Space Distribution Sensor Based on the Use of "General Elliptic Retarder Model", Optical Communications 2013 Conference, October 24-25, 2013, Prague, CZ, ISBN: 978-80-86742-37-3
5. [5] – Y.P. Miao and J. Q. Yao, Acta Phys. Sin. 62, 044223, 2013
6. [6] - Harneet V. Thakur, Sandipan M. Nalawade, Swati Gupta, Rohini Kitture, and S. N. Kale: Photonic crystal fiber injected with Fe<sub>3</sub>O<sub>4</sub> nanofluid for magnetic field detection, APPLIED PHYSICS LETTERS 99, 161 101-3 (2011)
7. [7] - R. Gao, Y. Jiang, and S. Abdelaziz: All-fiber magnetic field sensors based on magnetic fluid-filled photonic crystal fibres, , 2013 OPTICS LETTERS, Vol. 38, No. 9, May 1, 2013, 1539-1541
8. [8] - Y. Q. Yu, X. J. Li, X. M. Hong, Y. L. Deng, K. Y. Song, Y. F. Geng, H. F. Wei, and W. J. Tong, Opt. Express, 18, p. 15383, 2010
9. [9] - A. A. Kayani, K. Khoshmanesh, S. A. Ward, A. Mitchell, and K. Kalantar-zadeh, Biomicrofluidics 6, 031501 (2012).
10. [10] P. S. Westbrook, B. J. Eggleton, R. S. Windeler, A. Hale, T. A. Strasser, and G. L. Burdge, IEEE Photon. Technol. Lett. 12, 495 (2000).
11. [11] - A. Candiani, M. Konstantaki, W. Margulis, and S. Pissadakis: Optofluidic magnetometer developed in a microstructured optical fiber, OPTICS LETTERS, Vol. 37, No. 21, November 1, 2012